Steady-State Functional MRI Using Spoiled Small-Tip Fast Recovery Imaging

Hao Sun,[1]* Jeffrey A. Fessler,[1,2] Douglas C. Noll,[2] and Jon-Fredrik Nielsen[2]

Purpose: To determine whether a recently proposed steady-state magnetic resonance imaging (MRI) sequence, "small-tip fast recovery" (STFR), can be used for functional brain imaging. Compared to existing functional MRI (fMRI) based on T_2^*-contrast and long echo time, STFR has the potential for high-resolution imaging with reduced B_0 artifacts such as geometric distortions, blurring, or local signal dropout.

Methods: We used Monte Carlo Bloch simulations to calculate the voxel-averaged steady-state signal during rest and activation, for blood oxygen level dependent (BOLD) and STFR. STFR relies on a tailored "tip-up" radiofrequency pulse to align the spins with the longitudinal axis after each data readout segment, and here we performed proof-of-concept in vivo STFR fMRI experiments using a tip-up pulse tailored to a two-dimensional region-of-interest in motor cortex. Experiments were performed on multiple subjects to test reliability of the functional activation maps.

Results: Bloch simulations predict a detectable functional signal that depends mainly on intravoxel dephasing, and only weakly on spin diffusion. STFR produces similar activation maps and signal change as BOLD in finger-tapping experiments, and shows reliability comparable to BOLD.

Conclusion: STFR can produce functional contrast (even with short TE), and is a potential alternative to long-TE (T_2^*) fMRI. The functional contrast arises primarily from the interaction between T_2^*-like dephasing and the tailored tip-up pulse, and not from spin diffusion. **Magn Reson Med 73:536–543, 2015.**

Key words: functional magnetic resonance imaging; small-tip fast recovery; passband balanced steady-state free precession; passband steady-state free precession; blood oxygen level dependent

INTRODUCTION

The majority of functional magnetic resonance imaging (fMRI) studies in the brain use T_2^*-weighted gradient-echo (GRE) sequences with single-shot readout [blood oxygen level dependent (BOLD) fMRI] (1). The long echo time (TE) required to build up sufficient functional contrast makes BOLD fMRI susceptible to background B_0 inhomogeneity unrelated to oxygenation, leading to signal dropout near air/tissue boundaries and geometric distortions or blurring. Steady-state fMRI based on passband balanced steady-state free precession (passband bSSFP) uses segmented readouts and can produce high resolution functional maps with reduced geometric distortions (2–8), but is susceptible to dark "banding" artifacts in regions of high B_0 inhomogeneity and generally has lower functional contrast than BOLD (3).

Small-tip fast recovery (STFR) imaging is a recently proposed steady-state imaging sequence (9). STFR relies on a tailored "tip-up," or "fast recovery," radiofrequency (RF) pulse to align the spins with the longitudinal axis after each data readout segment, such that the magnetization is preserved for the next TR and a T_2 dependence is introduced. The design of the tip-up pulse is based on a separately acquired B_0 map. STFR can provide bSSFP-like image contrast, but with reduced signal variations due to B_0 inhomogeneity. However, it is not yet known whether STFR is suitable for fMRI, and whether the functional contrast mechanism is the same as in passband bSSFP.

Here, we investigate the possibility of using STFR for steady-state fMRI, using Monte Carlo Bloch simulations and proof-of-concept in vivo functional imaging experiments. We first review the STFR imaging concept, and discuss potential functional contrast mechanisms. We then describe our steady-state Monte Carlo Bloch simulations that account for spin diffusion in a realistic microvascular environment. We continue by describing our STFR functional experiments, including the design of the tailored tip-up RF pulse. Our results indicate that STFR can produce reliable functional contrast (even with near-zero TE), and that diffusion plays only a minor role.

THEORY

STFR Imaging

The STFR imaging principle is illustrated in Figure 1. As in most conventional imaging sequences, a tip-down pulse α is first played out, and the signal is acquired during a free precession interval of duration T_{free}. During this interval, the spin precesses in the transverse plane by an angle

$$\theta(\vec{r}) = \omega(\vec{r})T_{free}, \quad [1]$$

where $\omega(\vec{r})$ is the spatially varying local B_0 off-resonance frequency. After data readout, spins within the desired imaging region are tipped back toward the longitudinal axis (m_z) by a spatially tailored tip-up pulse $\beta(\vec{r})$ that depends on $\theta(\vec{r})$. The residual transverse magnetization remaining after the tip-up pulse can be spoiled using RF-

[1]Department of Electrical Engineering and Computer Science, University of Michigan, Ann Arbor, Michigan, USA.
[2]Department of Biomedical Engineering, University of Michigan, Ann Arbor, Michigan, USA.
Grant sponsor: National Institutes of Health; Grant numbers: R21EB012674, R01NS058576.
*Correspondence to: Hao Sun, Ph.D., Functional MRI Laboratory, 1073 B.I.R.B., 2360 Bonisteel Ave, Ann Arbor, MI 48109-2108. E-mail: sunhao@umich.edu
Received 13 October 2013; revised 29 December 2013; accepted 3 January 2014
DOI 10.1002/mrm.25146
Published online 11 March 2014 in Wiley Online Library (wileyonlinelibrary.com).

spoiling, i.e., by inserting an unbalanced gradient area and cycling the RF phase quadratically (10). RF-spoiling has the additional benefit that it suppresses signal from outside the field-of-view in the slice-select direction, and hence allows a thin slab (or slice) to be imaged by using a slab-selective tip-down pulse and a nonslice-selective tip-up pulse (9). The transverse magnetization for an isochromat is (9)

$$M_T = M_0 \sin\alpha \frac{e^{-T_g/T_1}(1 - e^{-T_{free}/T_1})\cos\beta + (1 - e^{-T_g/T_1})}{1 - e^{-T_g/T_1}e^{-T_{free}/T_2}\sin\alpha\sin\beta\cos(\theta_f - \phi) - e^{-T_g/T_1}e^{-T_{free}/T_1}\cos\alpha\cos\beta} \quad [2]$$

where T_{free} is the free procession time, T_g is the duration of the gradient crusher, ϕ is the phase of the tip-up pulse, and α and β are the flip angle of tip-down pulse and tip-up pulse, respectively. Based on this equation, when there is no phase mismatch ($\phi = \theta_f$), the transverse magnetization would be close to passband bSSFP [see plot in Ref. (9)]. Although STFR is a spoiled sequence, it still has T_2 dependence as the transverse magnetization recovered by the tip-up pulse is a function of T_2, and this magnetization will contribute to the final steady-state signal.

Possible Functional Contrast Mechanisms in STFR: Diffusion and T_2^*

Increased brain activation is generally assumed to be accompanied by reduced B_0 inhomogeneity within a voxel, due to decreased deoxyhemoglobin concentration resulting from overcompensatory arterial blood flow increases in response to increased oxygen demand (1). In conventional BOLD fMRI, these intravoxel inhomogeneity changes are detected as changes in T_2^* using single-shot imaging with long TE. In passband bSSFP, conversely, functional contrast is believed to be driven at least in part by the interaction between spin diffusion and intravoxel B_0 inhomogeneity: during activation, diffusion-related deviations in spin free precession angle between RF excitations are reduced, leading to a signal change that can be modeled as a change in "apparent" T_2 (6,8). The functional contrast mechanism is, therefore, (at least in part) decoupled from the choice of TE, enabling segmented readouts and hence reduced geometric distortions. Given the similarity between STFR and passband bSSFP (9), one might expect STFR to exhibit a similar diffusion-driven functional contrast.

In addition to spin diffusion, STFR has a second possible source of functional contrast, which arises from the dependence of the steady-state transverse magnetization on the mismatch between the spin phase after data readout (θ_f) and the phase (ϕ) of the tailored tip-up pulse (Fig. 1a). Figure 1b plots the transverse magnetization for a spin isochromat as a function of the phase mismatch $\theta_f - \phi$, using Eq. [2]. The tip-up pulse is tailored to the mean phase of spins within a voxel, therefore, different spins in a voxel experience different phase mismatch and the total voxel signal must be obtained by weighted integration of the isochromat signal profile over the B_0 distribution within a voxel (illustrated in Fig. 1b):

$$S(\vec{r}) = \int M_T(\theta_f - \phi(\vec{r}))f_{\vec{r}}(\theta_f)d\theta_f \quad [3]$$

where $\vec{r}$ is the voxel position, $f_{\vec{r}}(\theta_f)$ is the intravoxel phase distribution for a voxel at $\vec{r}$, which is often modeled as a Lorentzian distribution. It is, therefore, possible that the interaction between the activation-induced change in the intravoxel phase distribution and the tailored tip-up pulse can lead to a measurable signal change in spoiled STFR imaging.

It is not immediately clear (i) which of these mechanisms dominate and (ii) whether they are sufficient to produce detectable functional signal. In this article, we use numerical Bloch simulations and in vivo functional experiments to address these questions.

METHODS

Monte Carlo Bloch Simulations

To investigate the functional contrast behavior of STFR, we performed time-resolved Bloch simulations similar to those in Refs. (6) and (8). We constructed a 1-mm^3 numerical three-dimensional (3D) voxel model containing cylindrical vessels with random orientations. The simulated vessel diameters were in the range 5.6–60 μm (11). We assumed a constant blood fraction $f_b = 7.3\%$ (6), and venous oxygenation of 67 and 81% during rest and activation, respectively (12). We calculated the intravascular and extravascular field according to Eqs. [4–6] in Ref. (6). To keep memory requirements manageable, only a two-dimensional (2D) plane through the 3D numerical voxel was simulated, as in Ref. (6). Figure 2a shows the resulting 2D intravoxel B_0 field map.

We simulated the steady-state signals for STFR, both with and without diffusion. In each simulation, 2500 spins were randomly placed into the 2D numerical voxel. Spins were assigned a 2D random walk using diffusion coefficient of 0.001 mm^2/s with 50-μs simulation step size (6). We assumed circular voxel edge conditions (i.e., spins leaving the voxel at one edge were allowed to enter the voxel through the opposite edge). We used $T_1/T_2 = 1470/71$ ms in simulation (13). In the nondiffusion case, we fixed all spin locations and repeated the simulations. We simulated a range of TRs (8–24 ms) and flip angles (8–45°). We assumed nonselective 1.5 ms hard pulses, TE = 1.8 ms (to match our STFR experiments), and 1.2 ms gradient crusher for STFR. We ran the simulations for a duration of 5.5 × T_1 prior to "recording" the signal to establish a steady state.

For reference, we also simulated the spoiled GRE BOLD with 16° flip angle, 44 ms TR, and 32 ms TE, which is matched to our experiments. For computational efficiency, we assumed ideal RF spoiling for STFR and

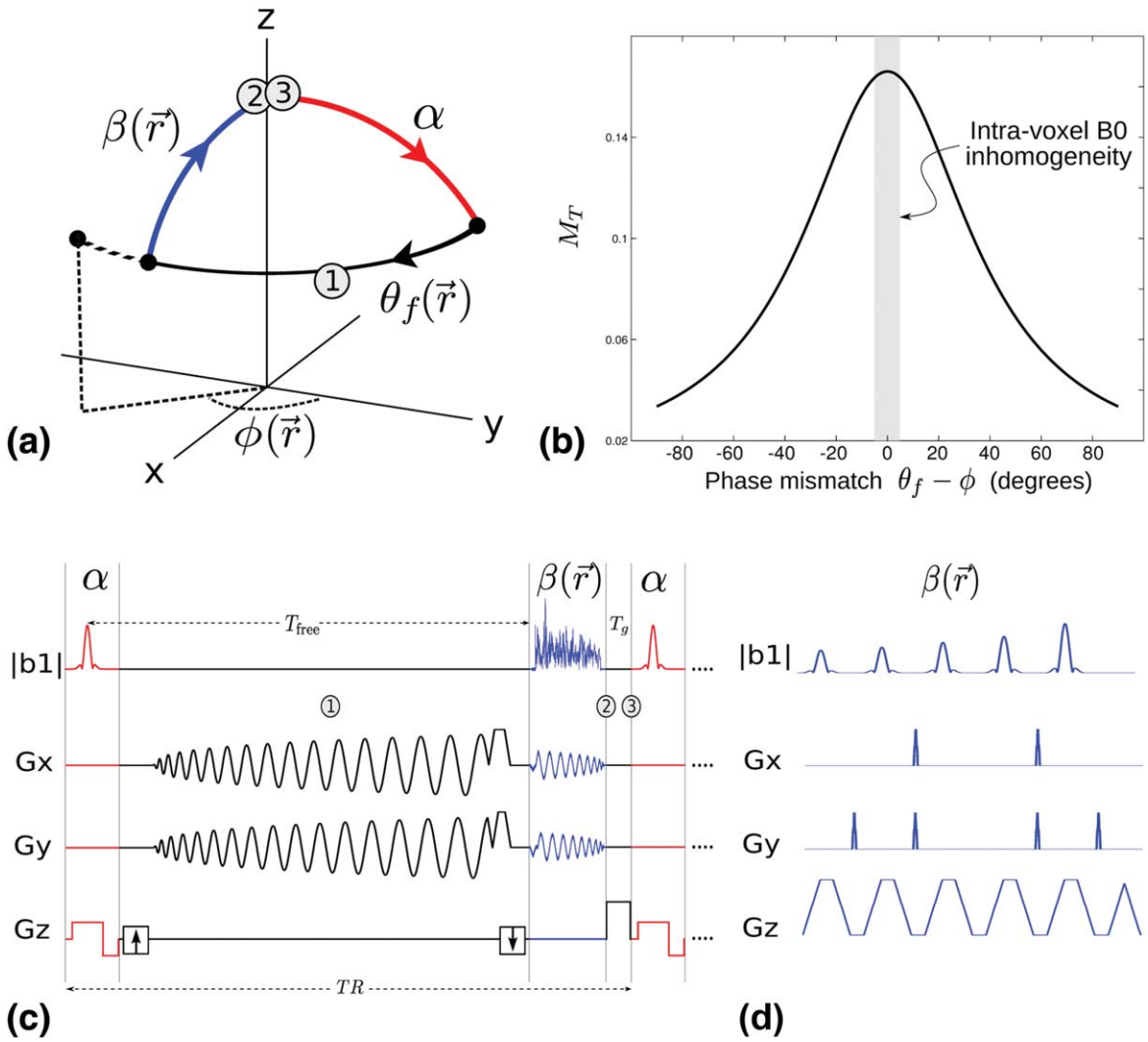

FIG. 1. Proposed STFR functional imaging sequence. **a**: Steady-state spin path for a single spin isochromat. The tip-up pulse (blue) is tailored to the local free precession angle. In general, there will be a mismatch $\theta_f - \phi$ between the spin phase at the end of the free precession interval (θ_f), and the phase (direction) of the tip-up pulse (ϕ). In STFR imaging, the goal is to design a tip-up pulse that minimizes $\theta_f - \phi$ within the ROI. **b**: Steady-state STFR transverse magnetization for a single spin isochromat as a function of phase mismatch $\theta_f - \phi$, calculated from Eq. [2]. The observed voxel-averaged signal is obtained by weighted integration of the signal profile over the B_0 distribution within a voxel (Eq. [3], illustrated with shaded gray column). **c**: Pulse sequence diagram for the STFR sequence used in the in vivo functional experiments (spiral tip-up pulse). **d**: fast-kz tailored tip-up pulse (only five subpulses are shown).

BOLD in the simulation, i.e., the transverse magnetization is set to 0 prior to each tip-down pulse. We implemented the Bloch simulator in MATLAB using C-mex files, available online (http://www.eecs.umich.edu/∼sunhao).

Functional Imaging

To establish whether STFR can produce useful functional contrast, we performed fMRI experiments in five healthy volunteers. Table 1 summarizes these experiments. We performed all imaging experiments on two different GE 3T scanners equipped with quadrature transmit/receive head coils. The subjects performed bilateral finger-tapping, using five cycles of a 20 s on, 20 s off, block paradigm. We used checkerboard visual stimulation to cue the subject to begin/end finger tapping.

We repeated the fMRI run 3–5 times for each subject, to quantitatively compare STFR and BOLD in terms of test-retest reliability (14,15). The number of repeated scans varied across subjects (from 3 to 5) depending on how long the volunteer could comfortably stay in the scanner. One subject was scanned in a second session to demonstrate: (1) the effect of varying flip angle and (2) the use of an alternative tip-up pulse design (spiral).

We acquired time-series image volumes using the sequence shown in Figure 1c,d, which consists of a 3-cm axial slab-selective Shinnar–Le Roux tip-down pulse (16), a balanced 3D stack-of-spirals readout, and a tailored tip-up pulse. Other sequence parameters were: 5 cm field-of-view with 10 partitions in z; eight spiral kx-ky segments supporting 128 × 128 matrix size; in-plane field-of-view 24 cm. To suppress out-of-slab steady-state signal formation (primarily a concern when using nonslice-selective

tip-up pulses such as spiral), we used RF-spoiling with 117° linear phase increment, as described in Ref. (9).

To minimize the possible influence of eddy-currents on the steady-state, we minimized the frequency of large jumps in k-space (caused, e.g., by rotating the spiral leafs) by acquiring all z partitions in linear fashion before moving to the next spiral leaf, and by alternating the direction of kz-space traversal, when jumping to the next spiral leaf (17,18).

In each scan session, we tailored the tip-up pulse to a 2D region-of-interest (ROI) containing most of the central slice, but excluding regions with severe B_0 inhomogeneity if present (such as the frontal sinus). To design the pulse, we acquired an axial 2D B_0 map $\omega(x,y)$ located at the center of the 3D fMRI image volume ($z=0$). We calculated the 2D B_0 map from two spoiled gradient-echo images with TE difference of 2.3 ms to minimize the contribution of fat to the measured image phase difference (flip angle 16°; 64 × 64 matrix size).

Table 1
Summary of fMRI Experiments

Subject	A, Session 1	A, Session 2	B to E
Region	Motor	Motor	Motor
Sequence(s)	STFR/BOLD	STFR	STFR/BOLD
No. repetitions	5	1	3–5
Tip-up pulse	fast-kz (7 ms)	spiral (4.5 ms)	fast-kz (7 ms)
TR (ms)	20.2/43.4	18	24/44
Frame rate (s)	1.62/3.47	1.44	1.92/3.52
TE (ms)	1.8/32	1.8	1.8/32
Flip-angle (°)	16/16	16 and 8	16/16
Results	Figures 3 and 4	Figure 5	Figure 4

We designed the tailored tip-up pulses using two different RF designs: fast-kz (19) and spiral. The fast-kz (spoke) pulse is longer and can be tailored to only relatively smooth in-plane phase patterns, but it has the advantage that there is no out-of-slice signal. The fast-kz

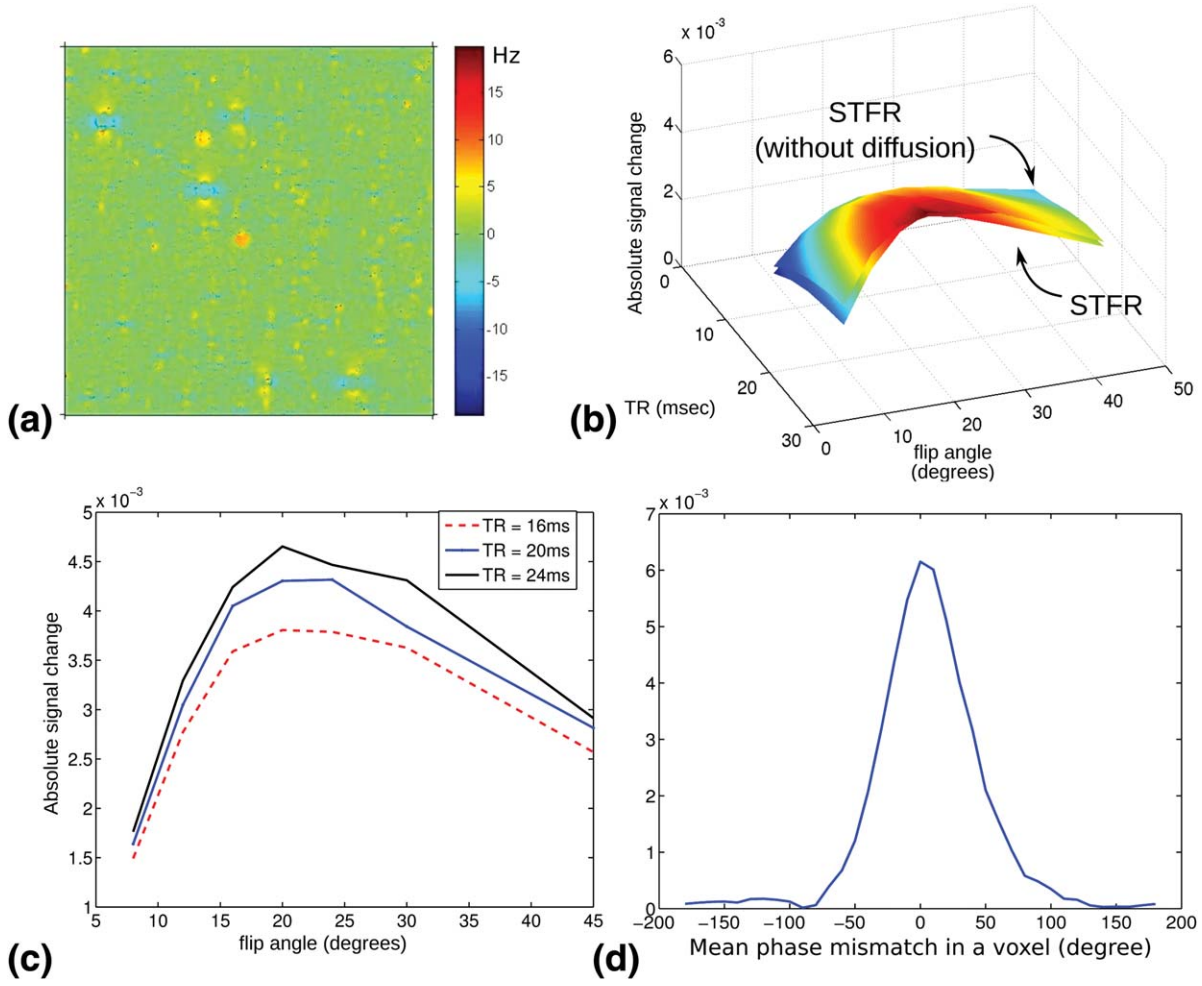

FIG. 2. Monte Carlo Bloch simulation results. **a**: Calculated microscopic B_0 inhomogeneity (Hz) in the numerical voxel used in our Monte Carlo Bloch simulations. A 2D cut through the 1 × 1 × 1 mm^3 voxel is shown. **b**: Absolute functional signal change for STFR over a range of TRs and flip angles with and without diffusion. **c**: Absolute functional signal change for STFR with respect to flip angle for several TRs used in our experiment. These simulations predict that STFR can produce a functional signal. The absolute signal change is maximized around 20°. "Turning off" spin diffusion has a relatively small impact on the functional signal, indicating that functional contrast in STFR arises primarily from the interaction between microscopic off-resonance and the tailored tip-up pulse, and not from spin diffusion. **d**: The absolute signal change when the mean phase mismatch in a voxel is not 0 (equivalent to the weighted integration over a narrow spectrum off the center in Fig. 1b). The functional signal change is maximized when mean phase mismatch for a voxel is 0.

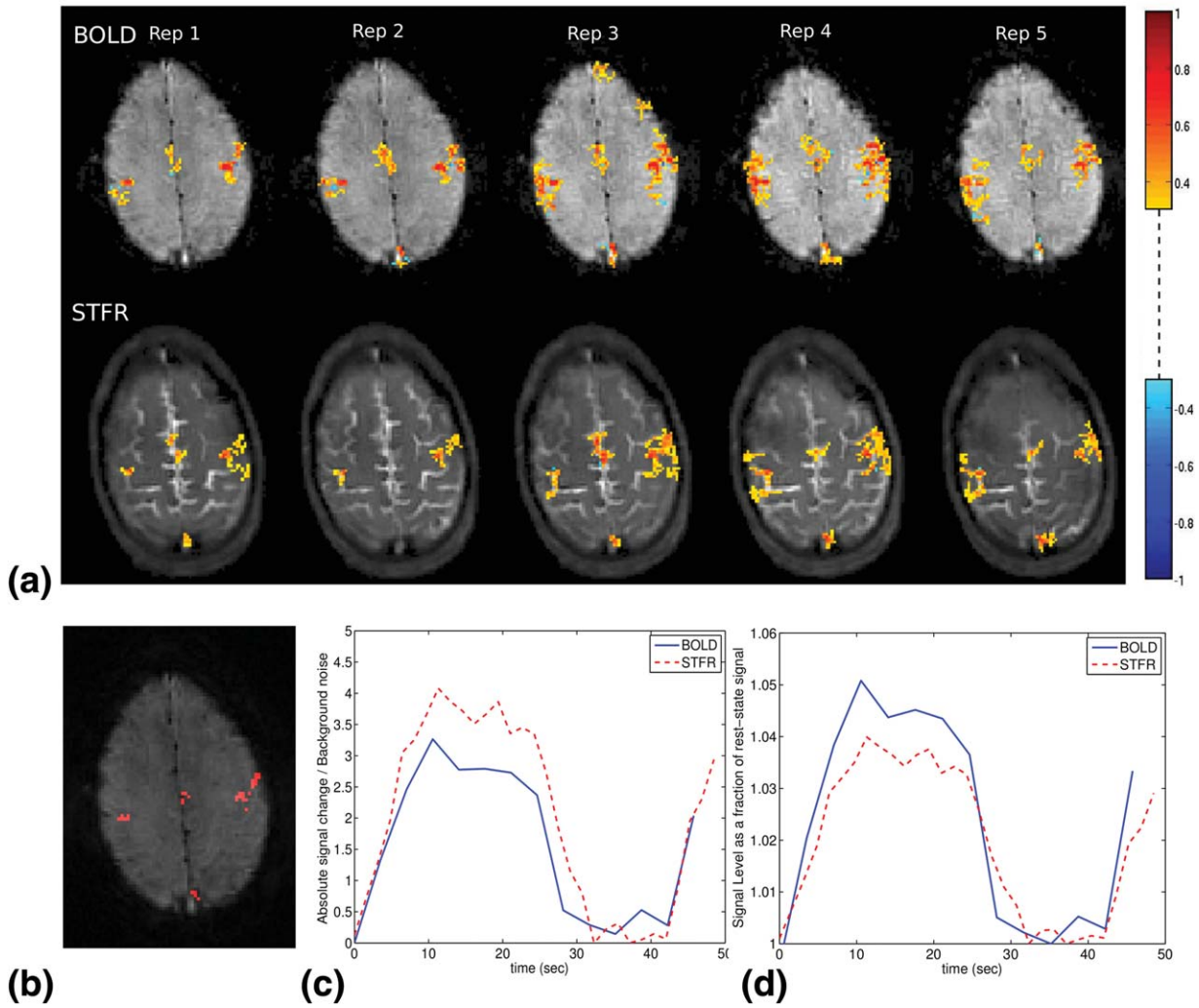

FIG. 3. Repeated motor cortex imaging using STFR and BOLD in one subject (A, Session 1). **a**: Activation maps with correlation threshold 0.3 and cluster size 10 (25). All five scans demonstrate that STFR can produce similar activation maps as BOLD, which are well localized to the motor cortex area. **b**: ROI used to calculate the mean time course for each sequence, obtained by selecting the pixels showing activations in at least four scans in both BOLD and STFR. **c**, **d**: One cycle of the mean time course signal over the ROI, shown as absolute (c) and relative (d) changes. In (c) the signal level is scaled by the corresponding background noise. In (d) the rest state signal is normalized to be 1. STFR has slightly lower relative signal change than BOLD, but higher absolute signal change (i.e., higher CNR), as predicted in simulation. The calculated functional signal change is reported in Table 2.

tailored tip-up pulse duration was 7 ms, and consisted of 10 slice-selective subpulses at different kx-ky locations. We designed the kx-ky locations and RF waveform jointly using a greedy approach as in Ref. (20). The spiral nonslice-selective tailored tip-up RF waveform was 4.5 ms, designed as in Ref. (9). We used the small-tip (Fourier) approximation (21) and the discretized design method in Ref. (22), implemented with the IRT MATLAB toolbox (http://www.eecs.umich.edu/~fessler). In our current experimental setting, after we acquire the B_0 map, the system will automatically trigger the pulse design code and then transfer the pulse to the scanner. The total overhead for the B_0 acquisitions and RF pulse creation was approximately 2 min.

We designed a 2D, rather than 3D, tip-up pulse to ensure accurate tip-up pulses in the center slice with acceptable pulse duration. Hence, these functional experiments were designed as proof-of-concept experiments, i.e., to investigate whether STFR can in fact produce functional contrast; a true 3D functional experiment would require a tip-up pulse tailored to a 3D ROI, which would extend the RF pulse duration significantly unless using transmit coil arrays. We also note that we could in principle have performed single-slice functional experiments for our purposes here; however, this could have introduced slice-profile errors and blood in-flow effects that could have confounded the results.

Table 2
Simulated and Measured Functional Signal Change

	Percent signal change (BOLD/STFR)	Absolute signal change (BOLD/STFR)
Simulation	5.2%/3.6%	0.9
Measurement	4.1%/3.1%	0.75

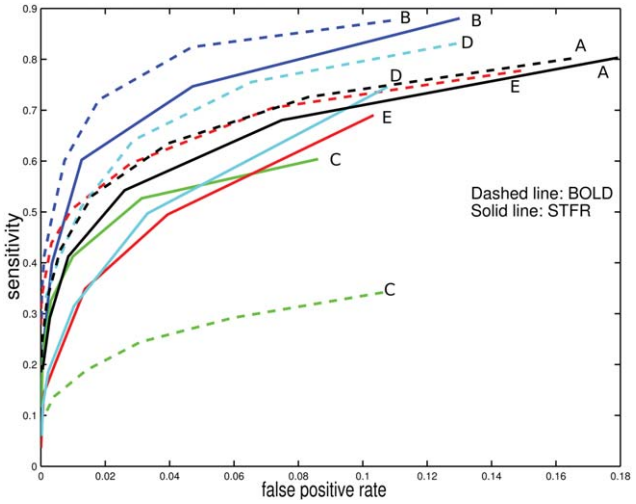

FIG. 4. Summary of test-retest reliability results for five different subjects (Subjects A–E), calculated using the method in Refs. (14) and (15) from motor cortex imaging data. The receiver operating characteristic curves for STFR are generally slightly lower than BOLD, but still demonstrate that it is a reliable sequence for detecting functional activity. One BOLD curve (C) is much lower than other curves, which is probably due to the motion artifact we observed in that set of data.

fMRI Processing and Analysis

We reconstructed 3D image volumes using iterative nonuniform fast Fourier transform (23,24) in the axial plane with second-order roughness penalty and no B_0 correction, and FFT in the through-slab (z) direction. The iterative algorithm was run for 15 iterations. We performed 2D image coregistration along the temporal dimension for each slice. We then applied linear time drift removal for each pixel. We correlated the resulting filtered time-series with the block stimulus to obtain a correlation value for each voxel.

We estimated test-retest reliability following (14,15). Specifically, this analysis is based on calculating activation maps using multiple activation thresholds, and obtaining a maximum likelihood estimate of sensitivity and false positive rate at each threshold. These rates are then plotted to form a receiver operating characteristic curve for each subject, which gives a quantitative reliability measure for each acquisition method (STFR and BOLD). The MATLAB code is available online (http://www.eecs.umich.edu/∼jfnielse).

RESULTS

Bloch Simulation Results

Figure 2 shows the simulated functional signal change for STFR (both with and without diffusion) over a range of TRs (8–24 ms) and flip angles (8–45°). Figure 2b shows the absolute signal change, i.e., as a fraction of M_0, over a range of TR and flip angles, which predicts that STFR can in fact produce a functional signal. Figure 2c shows the absolute signal versus flip angle for several TRs, to investigate the optimal flip angle for different TR. The absolute signal change is maximized around 20° flip angle, and increases with increasing TR. "Turning off" spin diffusion in the simulation has a relatively small impact on the functional signal, indicating that functional contrast in STFR is primarily driven by the interaction between microscopic off-resonance and the tailored tip-up pulse (as illustrated schematically in Figure 1b). As a reference, the simulated percent and absolute functional signal change of the spoiled gradient echo BOLD sequence (TR = 44 ms, TE = 32 ms, flip angle = 16°) is 5.2% and 0.0037, respectively. Note that the percent signal change of conventional BOLD is 44% higher than STFR with TR = 20 ms, flip angle = 16°, but the absolute signal change is 10% lower.

The simulation was performed assuming the tip-up pulse perfectly matches the mean accumulated phase of each voxel, which corresponds to a weighted integration over a narrow spectrum located in the center of Figure 1b. We also simulated the absolute signal change when the mean phase mismatch is not 0 (that would correspond to a weighted integration over a narrow spectrum off the center), and the result is shown in Figure 2d, which predicts that the functional signal change is maximized when mean phase mismatch is 0°.

Functional Imaging

Figure 3a shows the thresholded correlation maps of STFR and BOLD imaging for five scans in one subject (A, Session 1). Both STFR and BOLD show high correlation in the motor cortex areas. To quantitatively evaluate the functional signal, we first selected a ROI by choosing all the pixels that show activations in at least four scans in both STFR and BOLD (see Fig. 3b), and then obtained the signal time course for voxels within that ROI. The absolute signal change is shown in Figure 3c, which was obtained by normalizing each time course by its corresponding background noise, and then taking the mean within the ROI. The percent signal change is shown in Figure 3d. STFR shows slightly smaller percent signal change than BOLD, but larger absolute signal change, as predicted in simulation. The measured percent signal change is reported in Table 2, and is in good agreement with simulation results, scaled by an arbitrary factor (1.2 times). Also, the measured result agrees with the simulation prediction that STFR has higher absolute signal change than BOLD.

Figure 4 shows receiver operating characteristic curves for STFR and BOLD in five subjects (A–E). STFR functional imaging shows good reliability in general, but slightly lower than conventional BOLD. One BOLD curve had very low reliability, which may be due to motion artifact (observed in the functional maps for that subject).

Finally, Figure 5 shows STFR functional imaging results of one subject for two different flip angles (8 and 16°). Imaging with 16° flip angle results in more active voxels in the expected region compared to 8°. To quantitatively compare the results for different flip angles, we plotted the mean time course over an ROI in Figure 5c,d. The ROI is chosen by selecting the voxels that are classified as active in both flip angle acquisitions. Higher flip angle has more absolute and percent signal change, which agrees with the simulation.

DISCUSSION

The Bloch simulation results suggest that the STFR functional signal arises primarily from interactions between

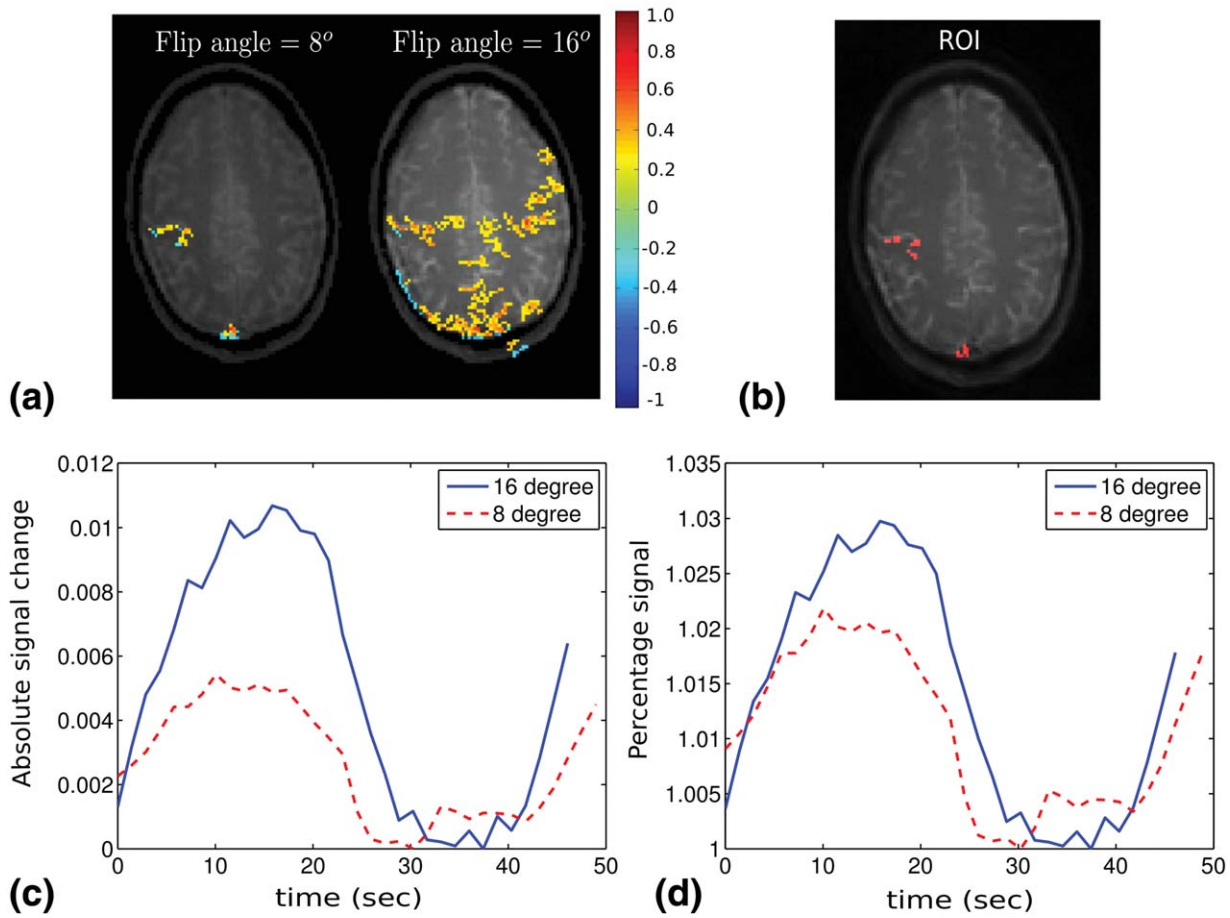

FIG. 5. Effect of flip angle on functional signal in STFR. **a**: Correlation map obtained with STFR fMRI, using flip angles 16 and 8°. Threshold and cluster size are 0.22/12 for both flip angle acquisitions. **b**: ROI used to calculate the mean time course for each flip angle, which includes pixels showing activation in both flip angle acquisitions. **c**, **d**: One cycle of mean time course within ROI. 16° flip angle produces higher absolute and percent functional signal change compared to 8° flip angle, as predicted in simulation.

the intravoxel dephasing and the tip-up pulse. If we ignore the relatively small diffusion effect, we can obtain the STFR functional signal by numerical weighted integration of the steady-state signal over the intravoxel frequency distribution as in Eq. [3], instead of performing a full Monte Carlo Bloch simulation. Using this method, we predict a 3.3% signal change, which is close to the Monte Carlo simulation result of 3.6%.

The dephasing effect in STFR is similar, but not exactly the same as the T_2^* effect in the conventional BOLD sequence. We can not simply replace T_2 in Eq. [2] with a conventionally defined T_2^*, i.e., $1/T_2^* = 1/T_2 + 2\pi\gamma$, where γ is the half-width at half-maximum of the intravoxel Lorentzian distribution, to obtain the voxel signal. Fitting a Lorentzian line shape to the simulated frequency distribution with $T_2 = 71$ ms (13) yields T_2^* values of 62 and 68 ms in rest and active conditions, respectively, (we have not found literature supporting those T_2^* values but we believe T_2^* change of this size is reasonable, as it would produce a ~4% BOLD functional change assuming TE = 30 ms, which is within the commonly observed range). By replacing T_2 with T_2^* in Eq. [2], we obtain a percentage signal change of 7.0%, which is almost twice the contrast obtained from Monte Carlo simulation or numerical integration, supporting the idea that the functional contrast mechanism is not quite the same as T_2^* decay. In addition, from Eq. [2], we note that T_2 is paired with T_{free}, not TE, which decouples the main source of functional signal from TE.

In our Monte Carlo Bloch simulations, we observed that the effect of diffusion is to increase the image signal and decrease the functional contrast compared to the result without diffusion (see Fig. 2). We think the reason for this change is that with diffusion, spins effectively experience different frequencies during the free precession interval, and that the accumulated phase, therefore, tends to be closer to the mean phase of that voxel. This effectively narrows the line spread of the intravoxel distribution, which increases the image signal but decreases the functional contrast.

Flip angle and TE are two other variables that affect the signal contrast. We used 16° in most of our experiments, which is approximately the Ernst angle for the BOLD acquisitions (assuming a T_1 of about 1.1 s). According to the simulation in Figure 2b, a flip angle around 20° generates the maximum absolute signal change. We used the minimum available TE for STFR in our experiments, but we found later in simulation that the functional signal increases with increasing TE (not

shown here), probably due to the normal T_2^* effect. This suggests that a spiral-in readout rather than a spiral-out readout could be used to increase the effective TE, and therefore, the functional signal.

Physiological fluctuations in B_0 (e.g., due to respiration) would shift the voxel signal as a whole along the curve in Figure 2d, which would reduce the functional contrast. We expect the B_0 shift due to respiration to be of order 1–2 Hz at 3T [fluctuations of 1.45–4 Hz have been reported at 7T (26)], which would not shift the voxel signal significantly (e.g., 5–11° assuming $T_{free} = 15\,ms$) along the curve in Figure 2d. In the experiments presented here, we have not observed significant physiological noise increases in STFR compared to BOLD.

A potential advantage of STFR compared to BOLD is that it can achieve high resolution segmented 3D imaging with reduced signal loss and image distortion. However, to achieve this across the whole brain, a 3D tailored tip-up pulse would be necessary, which may be prohibitively long. We have suggested methods for improving 3D tailored pulse design (27), but it is still challenging to tailor to the whole brain including regions with high field inhomogeneity (e.g., near frontal sinus). A potential solution is to use parallel transmission to reduce the pulse duration, and we plan to explore the feasibility of 3D STFR functional protocol using an 8-channel parallel transmit head array (28).

CONCLUSIONS

Taken together, the work presented here indicates that STFR has the potential to become a sensitive functional imaging modality. The functional contrast mechanism is decoupled from the TE, enabling segmented readouts and high image quality. Our Monte Carlo Bloch simulations indicate that STFR fMRI can produce observable functional contrast, and proof-of-concept in vivo STFR fMRI observations using a 2D tailored tip-up pulse support this prediction. Our simulations also indicate that the functional contrast in STFR is driven primarily by the interaction between microscopic off-resonance and the tailored tip-up pulse, and that diffusion plays a relatively minor role. In the future, we plan to evaluate the feasibility of whole-brain STFR fMRI, using 3D tailored tip-up pulses. We expect the design of such 3D pulses to benefit greatly from parallel transmission systems, high-order gradient shimming, and novel RF pulse design approaches.

ACKNOWLEDGMENT

The authors thank Daehyun Yoon for providing the fast-kz tailored pulse design code.

REFERENCES

1. Ogawa S, Tank DW, Menon R, Ellermann JM, Kim SG, Merkle H, Ugurbil K. Intrinsic signal changes accompanying sensory stimulation: functional brain mapping with magnetic resonance imaging. Proc Natl Acad Sci USA 1992;89:5951–5955.
2. Bowen C, Menon R, Gati J. High field balanced-SSFP FMRI: a BOLD technique with excellent tissue sensitivity and superior large vessel suppression. In Proceedings of the 13th Annual Meeting, Miami, Florida, USA, 2005. p. 119.
3. Zhong K, Leupold J, Hennig J, Speck O. Systematic investigation of balanced steady-state free precession for functional MRI in the human visual cortex at 3 Tesla. Magn Reson Med 2007;57:67–73.
4. Miller KL, Smith SM, Jezzard P, Wiggins GC, Wiggins CJ. Signal and noise characteristics of SSFP FMRI: a comparison with GRE at multiple field strengths. Neuroimage 2007;37:1227–1236.
5. Lee JH, Dumoulin SO, Saritas EU, Glover GH, Wandell BA, Nishimura DG, Pauly JM. Full-brain coverage and high-resolution imaging capabilities of passband b-SSFP fMRI at 3T. Magn Reson Med 2008;59:1099–1110.
6. Miller KL, Jezzard P. Modeling SSFP functional MRI contrast in the brain. Magn Reson Med 2008;60:661–73.
7. Muir ER, Duong TQ. Layer-specific functional and anatomical MRI of the retina with passband balanced SSFP. Magn Reson Med 2011;66:1416–1421.
8. Kim TS, Lee J, Lee JH, Glover GH, Pauly JM. Analysis of the BOLD characteristics in pass-band bSSFP fMRI. Int J Imaging Syst Technol 2012;22:23–32.
9. Nielsen JF, Yoon D, Noll DC. Small-tip fast recovery imaging using non-slice-selective tailored tip-up pulses and radiofrequency-spoiling. Magn Reson Med 2013;69:657–666.
10. Zur Y, Wood ML, Neuringer LJ. Spoiling of transverse magnetization in steady-state sequences. Magn Reson Med 1991;21:251–263.
11. Piechnik SK, Chiarelli PA, Jezzard P. Modelling vascular reactivity to investigate the bias of the relationship between cerebral blood volume and flow under CO2 manipulation. Neuroimage 2008;39:107–117.
12. Haacke E, Lai S, Reichenbach J, Kuppusamy K, Hoogenraad F, Takeichi H, Lin W. In vivo measurement of blood oxygen saturation using magnetic resonance imaging: a direct validation of the blood oxygen level-dependent concept in functional brain imaging. Hum Brain Mapp 1997;5:341–346.
13. Stanisz G, Odrobina E, Pun J, Escaravage M, Graham S, Bronskill M, Henkelman R. T1, T2 relaxation and magnetization transfer in tissue at 3T. Magn Reson Med 2005;54:507–512.
14. Genovese CR, Noll DC, Eddy WF. Estimating test-retest reliability in functional MR imaging I: statistical methodology. Magn Reson Med 1997;38:497–507.
15. Noll DC, Genovese CR, Nystron LE, Vazquez AL, Forman SD, Eddy WF, Cohen JD. Estimating test-retest reliability in functional MR imaging II: application to motor and cognitive activation studies. Magn Reson Med 1997;38:508–517.
16. Pauly J, Le Roux P, Nishimura D, Macovski A. Parameter relations for the Shinnar-Le Roux selective excitation pulse design algorithm. IEEE Trans Med Imaging 1991;10:53–65.
17. Bieri O, Markl M, Scheffler K. Analysis and compensation of eddy currents in balanced SSFP. Magn Reson Med 2005;54:129–137.
18. Nielsen JF, Nayak KS. Interleaved balanced SSFP imaging: artifact reduction using gradient waveform grouping. J Magn Reson Imaging 2009;29:745–750.
19. Saekho S, Yip C, Noll DC, Boada FE, Andrew Stenger V. Fast-kz three-dimensional tailored radiofrequency pulse for reduced B1 inhomogeneity. Magn Reson Med 2006;55:719–724.
20. Yoon D, Fessler JA, Gilbert AG, Noll DC. Fast joint design method for parallel excitation RF pulse and gradient waveforms considering off-resonance. Magn Reson Med 2012;68:278–285.
21. Pauly J, Nishimura D, Macovski A. A k-space analysis of small-tip-angle excitation. J Magn Reson 1989;81:43–56.
22. Yip CY, Fessler JA, Noll DC. Iterative RF pulse design for multidimensional, small-tip-angle selective excitation. Magn Reson Med 2005;54:908–917.
23. Fessler JA, Sutton BP. Nonuniform fast Fourier transforms using min-max interpolation. IEEE Trans Signal Process 2003;51:560–574.
24. Fessler JA, Lee S, Olafsson VT, Shi HR, Noll DC. Toeplitz-based iterative image reconstruction for MRI with correction for magnetic field inhomogeneity. IEEE Trans Signal Process 2005;53:3393–3402.
25. Forman SD, Cohen JD, Fitzgerald M, Eddy WF, Mintun MA, Noll DC. Improved assessment of significant change in functional magnetic resonance imaging (fMRI): use of a cluster size threshold. Magn Reson Med 1995;33:636–647.
26. Moortele VD, Pfeuffer J, Glover G, Ugurbil K, Hu X. Respiration-induced b0 fluctuations and their spatial distribution in the human brain at 7 tesla. Magn Reson Med 2002;47:888–895.
27. Sun H, Fessler JA, Noll D, Nielsen JF. Strategies for improved 3D small-tip fast recovery (STFR) imaging. Magn Reson Med 2014;72:389–398.
28. Hollingsworth N, Moody K, Nielsen JF, Noll D, McDougall M, Wright S. An eight channel transmit system for transmit SENSE at 3T. In Proceedings of the IEEE International Symposium on Biomedical Imaging, Chicago, Illinois, USA, 2011. pp. 775–778.